Korean J. Chem. Eng., **29**(4), 519-524 (2012)
DOI: 10.1007/s11814-011-0196-0

Visible up-conversion luminescence of $CaWO_4 : Er^{3+},Yb^{3+}$ and emission enhancement by tri-doping of Li^+ ions

Do-Hwan Kim*, Jeong Ho Ryu,†, Jun Ho Chung***, Jong Won Eun***, Kwang Bo Shim***, and Sung-Yong Cho***

*Department of Environmental Engineering, Chonnam National Univeristy, 77, Yongbong-ro, Gwangju 500-757, Korea
**Department of Materials Science and Engineering, Chungju National University,
50, Daehak-ro, Chungju-si, Chungbuk 380-702, Korea
***Department of Materials Science and Engineering, Hanyang University,
17, Haengdang-dong, Seongdong-gu, Seoul 133-791, Korea
(*Received 28 April 2011 • accepted 1 August 2011*)

Abstract–Er^{3+},Yb^{3+} co-doped $CaWO_4$ polycrystalline powders were prepared by a solid-state reaction and their up-conversion (UC) luminescence properties were investigated in detail. Under 980 nm laser excitation, $CaWO_4 : Er^{3+},Yb^{3+}$ powder exhibited green UC emission peaks at 530 and 550 nm, which were due to the transitions of Er^{3+} ($^2H_{11/2}$)→Er^{3+} ($^4I_{15/2}$) and Er^{3+} ($^4S_{3/2}$)→Er^{3+} ($^4I_{15/2}$), respectively. Effects of Li^+ tri-doping into $CaWO_4 : Er^{3+},Yb^{3+}$ were investigated. The introduction of Li^+ ions reduced the optimum calcinations temperature about 100 °C by a liquid-phase sintering process and the UC emission intensity was remarkably enhanced by Li^+ ions, which could be attributed to the lowering of the symmetry of the crystal field around Er^{3+} ions.

Key words: UC (Up-conversion) Luminescence, $CaWO_4 : Er^{3+},Yb^{3+}$, Solid-state Reaction Method, Li^+ Tri-doping

INTRODUCTION

Research on up-conversion (UC) luminescent materials has received considerable attention because of their applications in many advanced technology fields, such as three-dimensional display [1], photonics [2], up-conversion lasers [3], temperature sensors [4], DNA detection [5] and biolabels [6]. To fulfill the corresponding requirements in a range of application fields, various UC host materials have been developed and studied, such as single crystals, glasses, ceramics, and so on. [7-9]. To obtain highly efficient UC luminescent materials, host matrices with low phonon energies are required. Rare-earth (RE) doped fluoride materials have been widely studied because of their low phonon thresholds [10-12]. However, their physical properties such as chemical stability and mechanical strength are not as good as oxide host materials [13]. Therefore, it is significant to search for oxide host materials with high UC efficiency.

Tungstate is a very important family of oxide materials that have potential application in various fields, such as photoluminescence [14], microwave application [15], optical fibers [16], and electrochemical cells [17]. As a self-activating luminescent material, tungstate has a few advantages: high chemical stability, high X-ray absorption coefficient, high light yield, and low afterglow to luminescence [18]. Calcium tungstate ($CaWO_4$) has the scheelite structure, and it has received intense attention because of its technological importance as an inorganic scintillating material. $CaWO_4$ has high density (6.1 g/cm^3), high irradiation damage resistance, interesting excitonic luminescence, thermoluminescence, simulated Raman scattering behavior, and relatively low phonon threshold energy compared to other oxide materials [19,20]. The W^{6+} ions in $CaWO_4$ matrices have strong polarization induced by large electric charge and small radius, consequently, decrease symmetries, and enhance stark energy splitting of Er^{3+} ion in the crystal field [21]. Therefore, we can expect that $CaWO_4$ may be an efficient host material for UC luminescence.

Among RE ions, Er^{3+} ion is the most popular activator because it shows strong excited state absorption at 980 and 800 nm, which are emission wavelengths of low-cost semiconductor laser diodes [22,23]. However, the corresponding transitions have weak ground state absorption, notably at 980 nm. Hence, a sensitizer is indispensable to achieve high optical pumping efficiency. In fact, combined with the high absorption cross section of Yb^{3+} near 980 nm, Er^{3+} ion yields increased luminescence efficiency in Er^{3+},Yb^{3+} co-doped materials [24,25]. An efficient energy transfer (ET) often appears due to the large spectral overlap between the $^2F_{5/2}$-$^2F_{7/2}$ (Yb^{3+}) emission and the $^4I_{11/2}$-$^4I_{15/2}$ (Er^{3+}) absorption bands.

And also, it is well known that Li^+ dopant frequently plays important roles in morphology as well as in emission intensity of luminescent materials [26]. According to the quantum mechanical selection rules, the main intra-4f electronic-dipole transitions of RE ions are forbidden, which can be broken by the local crystal field of the RE ions due to the capability to intermix their f states with higher electronic configurations. Hence, the tailoring local environment of RE ions in the host lattice can be a promising route to enhance their optical performance [27]. Chen et al. reported that Li^+ ion co-doping into RE doped $BaTiO_3$ crystals decreased the crystal field symmetry, which led to greatly enhance the UC luminescence intensity [28].

Up to now, the UC luminescence properties in different host materials have widely been studied; however, the UC property of RE doped

†To whom correspondence should be addressed.
E-mail: jhryu@cjnu.ac.kr

$CaWO_4$ has not been studied in detail, to our knowledge. Therefore, realization of efficient NIR (near infra-red) to visible UC luminescence in $CaWO_4$ powder will have great impacts on its potential advantages. Here, we present a simple solid-state synthetic route for $CaWO_4 : Eu^{3+},Yb^{3+}$ powders and their UC luminescence properties. Moreover, effects of Li^+ doping on UC luminescence properties of the $CaWO_4 : Eu^{3+},Yb^{3+}$ were investigated in detail.

EXPERIMENTAL

In the present study, a solid-state reaction method [29,30] was adopted to prepare Eu^{3+},Yb^{3+} co-doped $CaWO_4$ ($CaWO_4 : Eu^{3+},Yb^{3+}$, labeled as "CW") and Li^+,Eu^{3+},Yb^{3+} tri-doped $CaWO_4$ ($CaWO_4 : Eu^{3+},Yb^{3+},Li^+$ labeled as "CWL") powder. All chemicals used were analytic-grade reagents without further purification. Nominal compositions of the two samples were 0.93 mol% of $CaCO_3$, 0.02 mol% of Er_2O_3, 0.05 mol% of Yb_2O_3, 1 mol% of H_2WO_4 for CW and 0.86 mol% of $CaCO_3$, 0.02 mol% of Er_2O_3, 0.05 mol% of Yb_2O_3, 0.035 mol% of Li_2CO_3, 1 mol% of H_2WO_4 for CWL sample, respectively. Starting materials were thoroughly mixed and ground for 1 hour. Subsequently, 10 g of the mixture was put into a corundum crucible and then calcined at 800, 900, 1,000 and 1,100 °C for 2 hrs in air. The crystalline phase of the calcined powders was identified by X-ray powder diffraction (XRD), operating at 40 kV using Cu-Kα radiation (λ=1.5406 Å). The powder morphology and microstructure were observed by scanning electron microscopy (SEM). UC luminescence spectra were recorded using a spectrophotometer in room temperature equipped with a laser diode of 100 mW and wavelength of 980 nm.

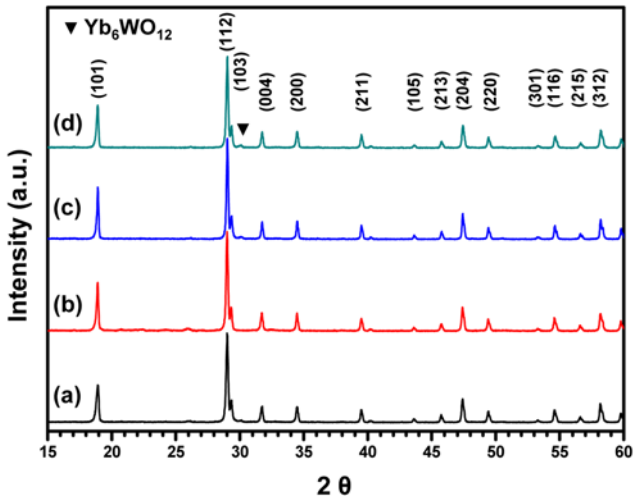

Fig. 1. XRD patterns of CW samples calcined at (a) 800, (b) 900, (c), 1,000 and (d) 1,100 °C for 2 hrs, respectively.

RESULTS AND DISCUSSION

Fig. 1 shows phase identifications of the CW samples calcined at (a) 800, (b) 900 (c) 1,000 and (d) 1,100 °C for 2 hrs, respectively. The $CaWO_4$ crystal exists in nature as scheelite-type tetragonal structure. At all calcination temperatures, most of the prominent peaks corresponding to scheelite-type $CaWO_4$ phase (JCPDS # 41-1431) were clearly observed in all the samples. RE tungstate characteristic peaks were not observed except very weak trace of Yb_6WO_{12}

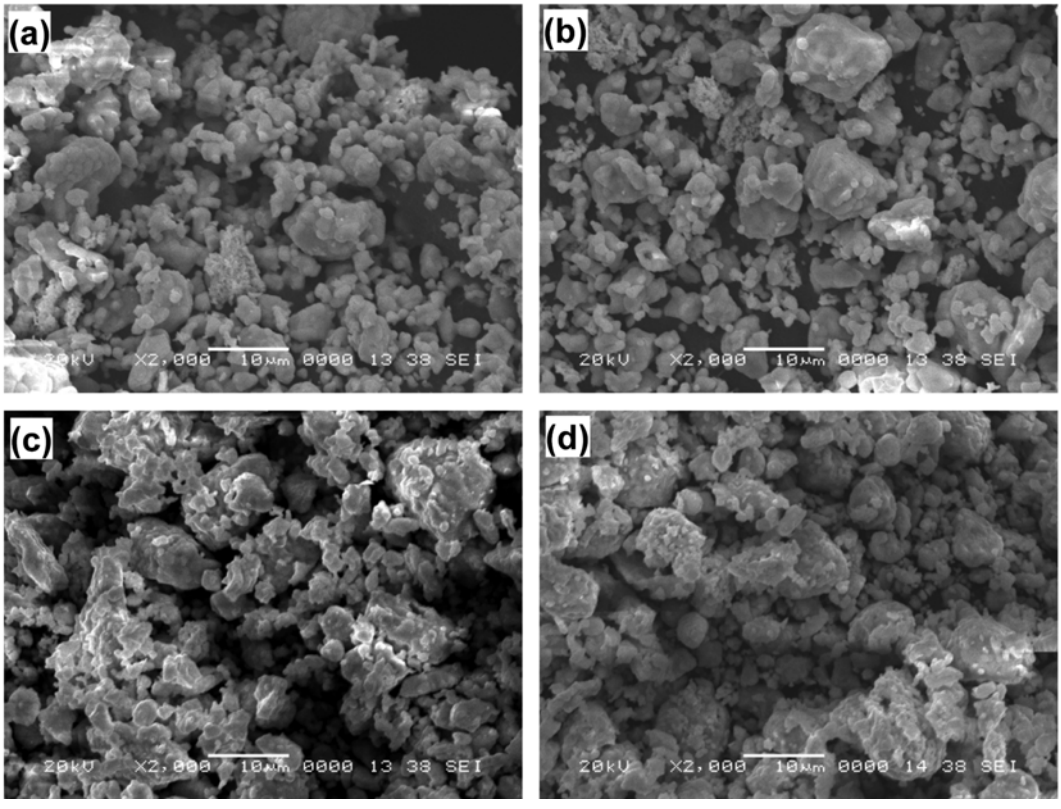

Fig. 2. SEM pictures of CW samples calcined at (a) 800, (b) 900, (c), 1,000 and (d) 1,100 °C for 2 hrs, respectively.

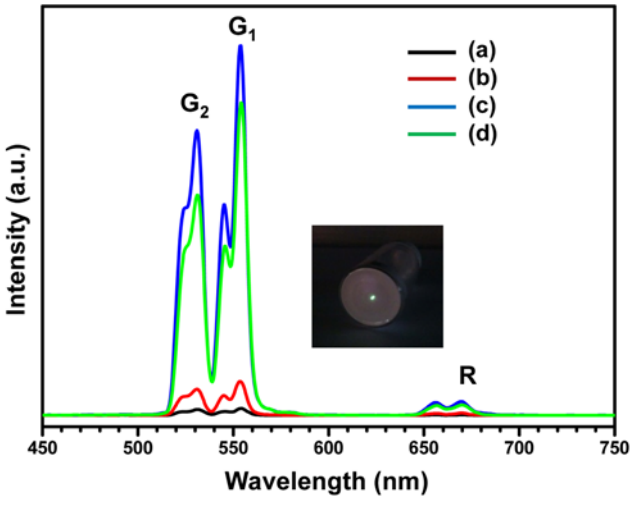

Fig. 3. UC luminescence spectra of CW samples calcined at (a) 800, (b) 900, (c), 1,000 and (d) 1,100 °C for 2 hrs excited by 980 nm laser diode. The photograph of inset shows the green emission of sample (c) observed by the naked eyes excited at 980 nm laser diode.

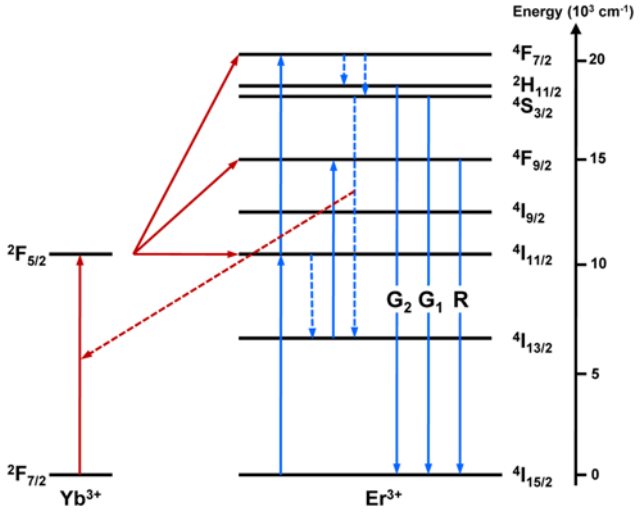

Fig. 4. The UC emission mechanism and population processes in CW and CWL samples.

upper 1,000 °C. With increasing calcination temperature from 800 to 1,000 °C, intensities of XRD peaks increased. However, at 1,100 °C, XRD intensity of the sample has no obvious differences compared to the sample of 1,000 °C, which confirms that the highest crystalline CW sample can be achieved at 1,000 °C via a solid-state reaction route. The diffraction peak shift was not detected, which means that lattice constant and crystal structure are not varied with calcination temperature. To investigate crystal growing process, we observed the morphology of the CW samples calcined at different temperatures. Fig. 2 shows SEM images of the CW samples heat-treated at (a) 800, (b) 900 (c) 1,000 and (d) 1,100 °C for 2 hrs, respectively. The CW sample calcined at 800 °C showed non-uniform morphology mixed with small particles less than 1 μm and aggregated big particles of 10 μm. There was obvious grain growth and particle aggregation with increasing temperature, and the sample (c) calcined at 1,000 °C showed uniform particle morphology with average size of about 3-5 μm.

Fig. 3 shows the UC luminescence spectra of the CW samples heat-treated at (a) 800, (b) 900 (c) 1,000 and (d) 1,100 °C under the 980 nm laser excitation. The UC luminescence spectra consisted of basically three regions: (1) the relatively weak red emission between 650 and 680 nm attributed to $^4F_{9/2} \rightarrow {}^4I_{15/2}$ transitions (R); (2) the intense green emission between 540 nm and 570 nm attributed to $^4S_{3/2} \rightarrow {}^4I_{15/2}$ transitions (G_1); and secondary green emissions between 515 to 540 nm assigned to $^2H_{11/2} \rightarrow {}^4I_{15/2}$ transitions (G_2). As shown in the UC spectral graph, the UC emission intensity increased with calcination temperature, and maximized at 1,000 °C. Eventually, we confirm that optimum olid-state reaction temperature for preparing CW powder with highest UC emission intensity is 1000 °C. This result is consistent with the optimum condition for highest XRD peak intensity of Fig. 1 and uniform powder morphology of Fig. 2(c). The CW sample calcined at 1,000 °C exhibited visible green emission by the naked eyes excited at 980 nm laser diode as shown in inset of Fig. 3.

The UC emission mechanism and population processes in Er^{3+},Yb^{3+}

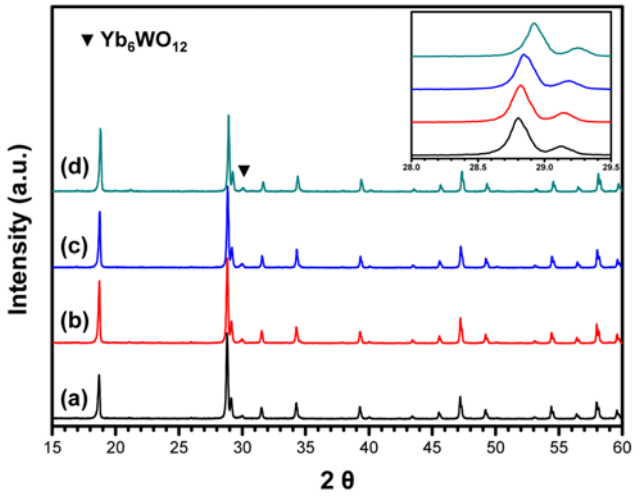

Fig. 5. XRD patterns of CWL samples calcined at (a) 800, (b) 900, (c), 1,000 and (d) 1,100 °C for 2 hrs, respectively. The inset details the shifts of (112) and (103) peak positions near 2θ= 29°.

co-doped systems are presented schematically in Fig. 4 [31]. First, the Er^{3+} ion is excited from the ground state $^4I_{11/2}$ to the excited state $^4I_{11/2}$. Subsequent nonradiative relaxations of $^4I_{11/2} \rightarrow {}^4I_{13/2}$ also populate the $^4I_{13/2}$ level. In the second-step excitation, the excited-state atoms are excited from the $^4I^{11/2}$ to the $^4F_{7/2}$ levels or from the $^4I_{13/2}$ to $^4F_{9/2}$ states. The populated $^4F_{7/2}$ may mostly nonradiatively relax to $^2H_{11/2}$ and $^4S_{3/2}$ levels, which produce two green UC emissions. The populated $^4F_{9/2}$ level causes red UC emissions.

Fig. 5 shows phase identifications of the CWL samples calcined at (a) 800, (b) 900 (c) 1,000 and (d) 1,100 °C for 2 hrs, respectively. The phase evolution process and the secondary phase (Yb_6WO_{12}) of the CWL samples were similar to the case of the CW samples. However, the highest XRD peak intensity was recorded at 900 °C, which means the optimum calcination temperature could be successfully decreased about 100 °C by addition of Li_2CO_3. Intermediate lithium-based secondary phase such as $Li_2W_5O_{16}$, Li_6WO_6 or

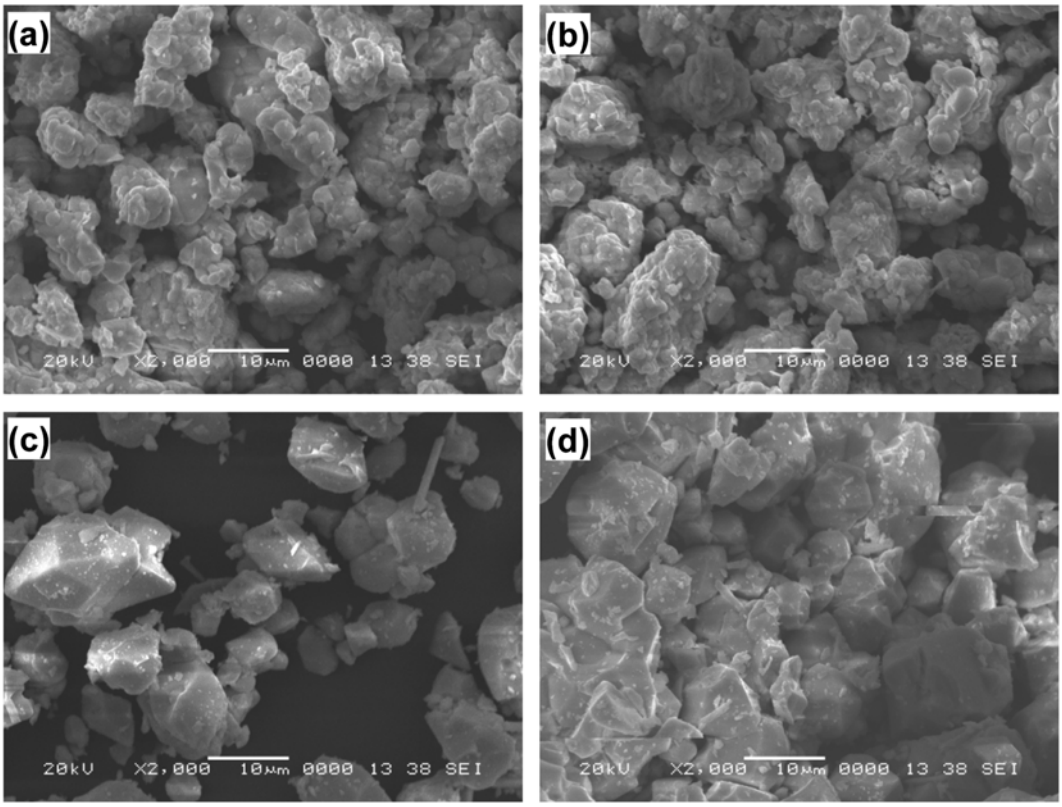

Fig. 6. SEM pictures of CWL samples calcined at (a) 800, (b) 900, (c), 1,000 and (d) 1,100 °C for 2 hrs, respectively.

$LiYbW_2O_8$ were not detected up to 1,100 °C. In CWL crystal, Er^{3+}, Yb^{3+} and Li^{+} ions occupy Ca^{2+} site because of the large charge difference between Ca^{2+} ion and W^{6+} ion. At the same time, Li^{+} ion could occupy the interstitial sites due to its small ionic size [32]. It is worth noting that when the Ca^{2+} ions is substituted by the Li^{+} ions with smaller ionic radius, the corresponding lattice constant becomes a little smaller. The inset of Fig. 5 shows the diffraction patterns near 2θ=29° shift to higher 2θ angle, which illustrate that more Li^{+} ions were doped into Ca^{2+} ion site, result to reduction of lattice constants.

Fig. 6 shows SEM images of the CWL samples calcined at (a) 800, (b) 900, (c) 1,000 and (d) 1,100 °C for 2 hrs, respectively. The crystal growth process and particle morphology change with increasing calcination temperature were similar to the case of CW powder. However, all the CWL samples calcined from 800 to 1,100 °C exhibited facet-shaped and well-grown particles compared to the CW powders. These SEM results confirmed that there exists a liquid-phase sintering process from 800 °C, which may be a result of formation of Li_2WO_4 (Li_2WO_4 melts around 730 °C) [33]. That is, the added Li_2CO_3 can act as flux to reduce the optimum calcinations temperature from 1,000 to 900 °C as shown in XRD of Fig. 5.

Fig. 7 shows the UC spectra of the prepared CWL samples calcined at (a) 800, (b) 900 (c) 1,000 and (d) 1,100 °C, respectively, under the 980 nm laser excitation. The UC emission intensity maximizes in the case of 900 °C and then decreases to 1,100 °C, which is consistent with optimum calcination condition for highest XRD peak intensity of Fig. 5. The upper inset of Fig. 7 depicts relative UC emission intensity of G_1 between CW and CWL samples with calcination temperatures. In the case of CWL sample prepared at

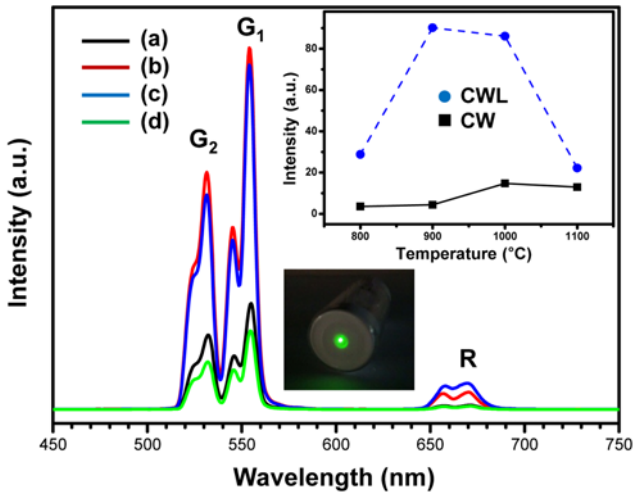

Fig. 7. UC luminescence spectra of CWL samples calcined at (a) 800, (b) 900, (c), 1,000 and (d) 1,100 °C for 2 hrs excited by 980 nm laser diode. The upper inset depicts change of relative UC emission intensities of CW and CWL samples with variable calcination temperatures. The photograph of lower inset shows the remarkably enhanced green emission of sample (b) observed by the naked eyes excited at 980 nm laser diode.

900 °C, the resultant enhancement of UC emission intensity was about six-times more than that of CW sample prepared at 1,000 °C. The CWL sample calcined at 900 °C exhibited much brighter green emission than CW sample as shown in lower inset of Fig. 7.

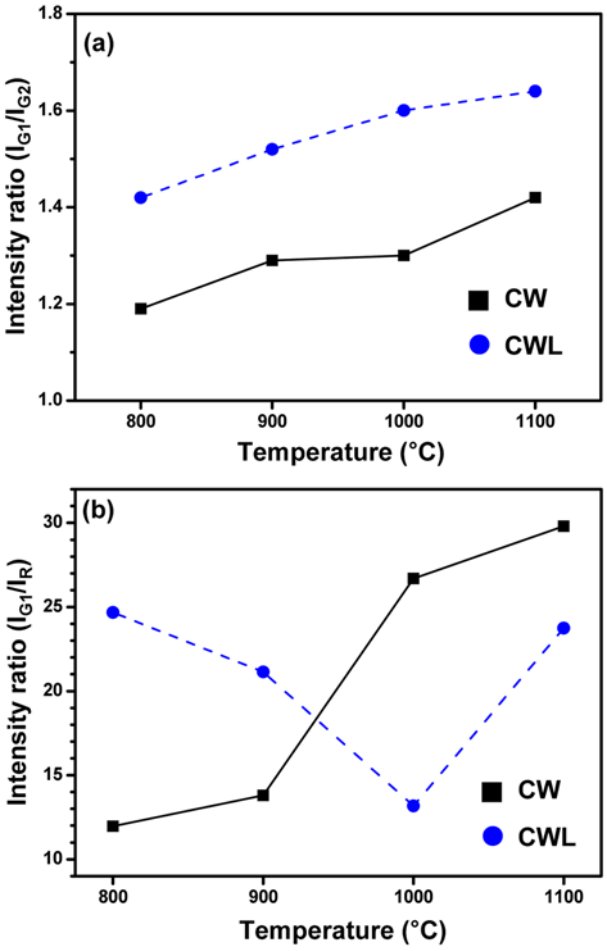

Fig. 8. The relative UC emission intensities, (a) I_{G1}/I_{G2} and (b) I_{G1}/I_R for the CW and CWL samples prepared at different temperatures.

Fig. 8 shows variations of relative UC emission intensity ratios (I_{G1}/I_{G2} and I_{G1}/I_R) of CW and CWL samples calcined at different temperatures. The I_{G1}/I_{G2} of CW sample calcined at 800 °C was 1.19 and increased to 1.42 at 1,100 °C as shown in (a). And also, the I_{G1}/I_R increased as the calcination temperatures. The I_{G1}/I_R value of CW sample at 1,000 °C was 26.69, which was much larger than that of $Y_2O_2S : Er^{3+},Yb^{3+}$ (I_{G1}/I_R at =2.0 [34]). As for the CWL sample, it exhibits weaker G_2 emission and stronger R emission with respect to the calcination temperature. The I_{G1}/I_{G2} ratios of CWL samples are larger than those of the CW samples at the same calcination temperature. However, I_{G1}/I_R ratio of CWL samples exhibits an abnormal drop from 24.68 at 800 °C to 13.17 at 1,000 °C.

It is well known that UC emission efficiency is determined by the nonradiative relaxation (ω_p) and increase in ω_p leads to low UC luminescence efficiency. The ω_p is influenced by the energy gap to the next-lower-lying of the activator Er^{3+} (ΔE), the lattice phonon energy of the host (ω), the site symmetry of the activator ions in the host matrix, and the ion-lattice interaction according to Miyakawa-Dexter equation [35]:

$$\omega_p = \omega_0 \exp\left(-\frac{\alpha \Delta E}{\hbar \omega}\right) \quad (1)$$

where α and ω_0 are host-dependent constants. We can expect ω in CW and CWL to be approximately equivalent and it does not obviously influence the UC emission efficiency in CW or CWL samples. Both the coordination number and the symmetry of O^{2-} ions around Er^{3+} affect the crystal field around Er^{3+}, which in turn influences the Stark splitting of the 4f levels in Er^{3+} by producing changes of symmetry and vibrational modes around the luminescence centers, resulting in a change of the oscillator strength between multiplets. Moreover, due to the highly charged (+6) and small ionic radius (0.62 Å), W ions strongly attract the oxygen ion, resulting in larger polarization, thus leading to a weak crystal field and larger distortion in the [CaO_8] polyhedron.

In doped $CaWO_4$, the Er^{3+} and Yb^{3+} ions act as the luminescence centers and the Li^+ ions as charge compensators. Er^{3+} and Yb^{3+} ions should occupy Ca^{2+} sites in positions of tetrahedral local symmetry, leading to formation of an [ErO_8] center. Li^+ ions may occupy the Ca^{2+} sites in $CaWO_4$ lattice in or near [ErO_8]. Li_{Ca} will not destroy the structure of the [ErO_8], but it will lead to some relaxation of the lattice and slight distortion of the [ErO_8] coordination, resulting in a lowering of the local symmetry of the crystal field around Er^{3+}. Thus the crystal field splitting becomes larger, which shifts the barycenter of the 4f level to slightly lower energy, leading then to the decrease of ΔE ($^2H_{11/2} \rightarrow {}^4S_{3/2}$) and ΔE ($^4S_{2/3} \rightarrow {}^4F_{9/2}$), which promotes the nonradiative relaxation $^2H_{11/2} \rightarrow {}^4S_{3/2}$ and $^4S_{3/2} \rightarrow {}^4F_{9/2}$ according to Eq. (1). Therefore, the $^2H_{11/2} \rightarrow {}^4I_{15/2}$ transitions (G_2) of Er^{3+} ions decrease while $^4F_{9/2} \rightarrow {}^4I_{15/2}$ transitions (R) increase as shown in Fig. 8.

CONCLUSIONS

$CaWO_4 : Er^{3+},Yb^{3+}$ (CW) and Li^+ tri-doped $CaWO_4 : Er^{3+},Yb^{3+}$ (CWL) powders were prepared by a conventional solid-state reaction method. The prepared CW and CWL powders exhibited bright green up-conversion (UC) luminescence under excitation of 980 nm laser. It was found that the UC emission intensity depends on the calcinations temperature, and the optimum calcination temperatures for highest UC luminescence were 1,000 and 900 °C for CW and CWL, respectively. Introduction of Li^+ ions not only promoted the crystal growing process but also enhanced remarkably UC luminescence intensity more than by six times. Moreover, Li^+ doping affected the UC luminescence spectra, the $^2H_{11/2} \rightarrow {}^4I_{15/2}$ transitions decreased while $^4F_{9/2} \rightarrow {}^4I_{15/2}$ transitions increased by Li^+-doping, which could be attributed to the lowering of the local symmetry of the crystal field around Er^{3+} ions.

NOMENCLATURE

UC : up-conversion
RE : rare-earth
CW : $CaWO_4 : Eu^{3+},Yb^{3+}$
CWL : $CaWO_4 : Eu^{3+},Yb^{3+},Li^+$
NIR : near infra-red
XRD : X-ray powder diffraction
SEM : scanning electron microscopy
JCPDS : joint committee for powder diffraction studies
2θ : Bragg angle of the X-ray diffraction peak [degree]
G_1 : green emission of Er^{3+} ions assigned to the $^4S_{3/2} \rightarrow {}^4I_{15/2}$ transitions

G_2 : green emission of Er^{3+} ions assigned $^2H_{11/2} \rightarrow {}^4I_{15/2}$ transitions
R : red emission of Er^{3+} ions assigned to $^4F_{9/2} \rightarrow {}^4I_{15/2}$ transitions

REFERENCES

1. E. Dowing, L. Hesselink, J. Ralston and R. Macfarlane, *Science*, **273**, 1185 (1996).
2. G. Y. Chen, Y. Liu, Y. G. Zhang, G. Somefalean, Z. G. Zhang, Q. Sun and F. P. Wang, *Appl. Phys. Lett.*, **91**, 133103 (2007).
3. F. Liu, E. Ma, D. Q. Chen, Y. L. Yu and Y. S. Wang, *J. Phys. Chem.*, **B110**, 20843 (2006).
4. X. Wang, X. G. Kong, Y. Yu, Y. J. Sun and H. Zhang, *J. Phys. Chem.*, **C111**, 15119 (2007).
5. L. Y. Wang and Y. D. Li, *Chem. Commun.*, **16**, 2557 (2006).
6. F. Vetrone, J. C. Boyer, J. A. Capobianco, A. Speghini and M. Bettinelli, *J. Phys. Chem.*, **B106**, 8622 (2002).
7. M. Takahashi, M. Lzuki, F. Kanno and Y. Kawamoto, *J. Appl. Phys.*, **83**, 3920 (1998).
8. J. Zhou, F. Moshary, B. M. Gross, M. F. Aark and G. A. Ahmed, *J. Appl. Phys.*, **96**, 237 (2004).
9. A. S. Gercia, R. Serna, M. J. Castrc and C. N. Afonso, *Appl. Phys. Lett.*, **84**, 2151 (2004).
10. S. Heer, K. Kömpe, H. U. Güdel and M. Haase, *Adv. Mater.*, **16**, 2102 (2004).
11. C. Liu and D. Chen, *J. Mater. Chem.*, **17**, 3875 (2007).
12. O. Ehlert, R. Thomann, M. Darbandi and T. Nann, *ACS Nano*, **2**, 120 (2008).
13. F. Wang and X. Liu, *Chem. Soc. Rev.*, **38**, 976 (2009).
14. L. Bardelli, M. Bini and P. Bizzeti, *Nucl. Instrum. Meth.*, **A569**, 743 (2006).
15. L. Uitert and S. Preziosi, *J. Appl. Phys.*, **33**, 2908 (1962).
16. H. Wang, F. Medina, Y. Zhou and Q. Zhang, *Phys. Rev.*, **B45**, 10356 (1992).
17. D. Y. Kim, S. Kim, M.-K. Yeo, I.-G. Jung and M. Kang, *Korean J. Chem. Eng.*, **26**, 261 (2009).
18. Z. Lou, J. Hao and M. Cocivera, *J. Lumin.*, **99**, 349 (2002).
19. M. J. Treadaway and R. C. Powell, *J. Chem. Phys.*, **61**, 4003 (1974).
20. R. Grasser, A. Scharmann and K.-R. Strack, *J. Lumin.*, **27**, 263 (1982).
21. L. F. Johnson and R. A. Thomas, *Phys. Rev.*, **131**, 2038 (1963).
22. F. Vetrone, J. C. Boyer, J. A. Capobianco, A. Speghini and M. Bettinelli, *Chem. Mater.*, **15**, 2737 (2003).
23. P. Gerner and H. U. Güdel, *Chem. Phys. Lett.*, **413**, 105 (2005).
24. F. Vetrone, J. C. Boyer, J. A. Capobianco, A. Speghini and M. Bettinelli, *J. Phys. Chem.*, **B107**, 1107 (2003).
25. H. Guo, N. Dong, M. Yin, W. Zhang, L. Loua and S. Xia, *J. Alloy. Compd.*, **415**, 280 (2006).
26. T. Hatayama, S. Fukumoto and S. Ibuki, *Jpn. J. Appl. Phys.*, **31**, 3383 (1992).
27. G. Chen, H. Liu, H. Liang, G. Somesfalean and Z. Zhang, *J. Phys. Chem.*, **C112**, 12030 (2008).
28. X. Chen, Z. Liu, Q. Sun, M. Ye and F. Wang, *Opt. Comm.*, **284**, 2046 (2011).
29. M.-J. Yoon, J.-H. In, H.-C. Lee and C.-H. Lee, *Korean J. Chem. Eng.*, **23**, 842 (2006).
30. Y. Wang, Y. Chen, S. Cheng and L. He, *Korean J. Chem. Eng.*, **28**, 964 (2011).
31. Q. Dai, H. Song, X. Ren, S. Lu, G. Pan, X. Bai, B. Dong, R. Qin, X. Qu and H. Zhang, *J. Phys. Chem.*, **C112**, 19694 (2008).
32. R. D. Shannon, *Acta Cryst.*, **A32**, 751 (1976).
33. X.-X. Luo and W.-H. Cao, *J. Mater. Res.*, **23**, 2078 (2008).
34. X. X. Luo and W. H. Cao, *Sci. China Ser. B-Chem.*, **50**, 505 (2007).
35. L. A. Riseberg and H. W. Moos, *Phys. Rev.*, **174**, 429 (1968).